PNAS

Supporting Information for

Nuclear VCP drives colorectal cancer progression by promoting fatty acid oxidation

Youwei Huang[a,b,c,1], Fang Wang[a,1], Xi Lin[a,1], Qing Li[a], Yuli Lu[a,d], Jiayu Zhang[e], Xi Shen[a], Jingyi Tan[c], Zixi Qin[a], Jiahong Chen[a,f], Xueqin Chen[a], Guopeng Pan[a], Xiangyu Wang[a], Yuequan Zeng[a], Shangqi Yang[a], Jun Liu[a], Fan Xing[g,*], Kai Li[e,*] and Haipeng Zhang[a,*]

[a]Department of Pharmacology, School of Medicine, Jinan University, Guangzhou, Guangdong 510632, China

[b]Guangdong Provincial Key Laboratory of Tumor Interventional Diagnosis and Treatment, Zhuhai Institute of Translational Medicine, Zhuhai People's Hospital Affiliated with Jinan University, Jinan University, Zhuhai, Guangdong 519000, China

[c]Biomedical Translational Research Institute, Health Science Center (School of Medicine), Jinan University, Guangzhou, Guangdong 510632, China

[d]Department of Public Health, Shantou Center for Disease Control and Prevention, Shantou, Guangdong 515000, China

[e]Guangdong Research Institute of Gastroenterology, The Sixth Affiliated Hospital of Sun Yat-sen University, Guangzhou, Guangdong 510655, China

[f]Department of Pathophysiology, School of Basic Medical Sciences, Peking University, Beijing 100191, China

[g]Medical Research Institute, Guangdong Provincial People's Hospital (Guangdong Academy of Medical Sciences), Southern Medical University, Guangzhou, Guangdong 510080, China

[1]These authors contributed equally to this work.

[*]To whom correspondence may be addressed. Address correspondence to: Haipeng Zhang, School of Medicine, Jinan University, 601 West Huangpu Avenue, Guangzhou, 510632, China. Email: zhanghp@jnu.edu.cn (H.Z.). Or to Kai Li, Guangdong Research Institute of Gastroenterology, The Sixth Affiliated Hospital of Sun Yat-sen University, 26 Erheng Road, Yuancun, Guangzhou, 510655, China. Email: likai39@mail.sysu.edu.cn (K.L.). Or to Fan Xing, Medical Research Institute, Guangdong Provincial People's Hospital (Guangdong Academy of Medical Sciences), Southern Medical University, 106 Zhongshan second road, Guangzhou, 510080, China. Email: xingfan@gdph.org.cn (F.X.).

This PDF file includes:

SI Materials and Methods

Fig. S1 to S9

Table S1 to S4

SI References

SI Appendix, Materials and Methods

Cell lines. HCT116 and HEK 293T cells were cultured in Dulbecco's modified Eagle's medium (DMEM), and DLD1 and HCT-8 cells were cultured in RPMI 1640. Both media were supplemented with 10% fetal bovine serum (FBS) and 1 × penicillin/streptomycin. All cultures were maintained in a humidified tissue culture incubator at 37℃ in 5% CO_2.

Plasmids and constructs. Human VCP, $VCP^{\triangle NLS}$ (lacking 60-66 amino acids), VCP^{K251A} (K251A mutation), and VCP^{K524A} (K524A mutation) were subcloned into the pCMV-3 × Flag-Puro vector. Human VCP shRNA (shVCP-1 and shVCP-2) and scrambled control shRNA were subcloned into pLenti-Tet-On-Puro. Sel1L sgRNA was cloned into the pLenti-spgRNA V2.0-spCas9-Blasticidin vector. Luciferase was then subcloned into the pLOV-blasticidin vector. Plasmids were purchased from OBiO Technology (Shanghai, China). pcDNA3.1(+)-HA and pcDNA3.1(+)-HA-ubiquitin were provided by Prof. Mong-Hong Lee. HDAC1 was subcloned into the pCMV-3 × Flag and pCMV-HA vector. The CPT1A promoter was subcloned into the pGL4.1 vector. All plasmids and mutations were confirmed by sequencing. The sequence information for the shRNA and gRNA used in this study is presented in *SI Appendix*, Table S1.

Animals. Female BALB/c-Nude mice of 4-6-week-old were purchased from GemPharmatech Co. (Jiangsu, China), and female B-NDG mice of 4-6-week-old were purchased from Biocytogen Pharmaceuticals Co. (Beijing, China). HCT116 cells stably expressing luciferase complemented with VCP or control vector (5×10^6 cells per mouse) were injected subcutaneously into nude mice. Tumor size was measured every two days, and tumor volume was estimated using the following formula: length × $width^2/2$. At the end of the experiment (day 15), mice were administered intraperitoneal injections of 50 mg/kg luciferin (Promega, P1041) and anesthetized with 2.5% isoflurane (RWD LIFE SCIENCE, R510). Ten minutes after injection, the mice were imaged using the IVIS Spectrum imaging system (PerkinElmer) and Living Image software. After imaging, the mice were euthanized and tumors were collected.

For the VCP inhibitor/metformin combination treatment, nude mice were injected subcutaneously with luciferase-expressing HCT116 cells (5×10^6 cells per mouse). When the tumor size reached 100-150 mm^3 (at day 7), mice were randomly assigned to four experimental groups. The treatment protocols are indicated in the Figure 6. CB-5083 (Selleck Chemicals,

S8101), metformin (Sigma, PHR1084) or a combination were administered by oral gavage. Tumor growth was measured at the indicated time points. At the end of the experiment (tumors were developed to ~1,000 mm^3 in the vehicle group on day 23), the tumor size was measured using bioluminescence as described above. After imaging, the mice were euthanized, and tumors were collected.

Two patient-derived xenograft (PDX) models were obtained from Prof. Mong-Hong Lee, and the protocols for the establishment of PDX models were as described previously(1). When the tumor size reached approximately 100-150 mm^3, mice were randomly assigned to four treatment groups. The treatment protocols are indicated in the Figure 6. CB-5083 (Selleck Chemicals, S8101), metformin (Sigma, PHR1084) or a combination were administered by oral gavage. Tumor growth was measured every three days. At the end of the experiment (tumors were developed to ~1,500mm^3 in the vehicle group), mice were euthanized, and tumors were collected.

Lentiviral production and infection. Lentiviral pSLenti vectors encoding VCP, $VCP^{\triangle NLS}$, VCP^{K251A}, or VCP^{K524A}, lentiviral pLOV vector encoding luciferase, lentiviral pLenti-Tet-On vectors encoding dox-inducible shRNA targeting VCP, and lentiviral pLenti-spgRNA-hspCas9 vector encoding sgRNA targeting Sel1L were obtained from OBiO Technology (Shanghai, China). Lentiviruses were produced in 293T cells using the Lenti-Pac HIV Expression Packaging Kit (GeneCopoeia, LT001) according to the manufacturer's instructions. Virus infection was performed by incubating cells with medium containing the indicated virus and 5 μg/ml polybrene (Sigma, TR-1003) for 24 h. Cells were allowed to recover in complete medium for 24 h or 48 h and then selected with 1 μg/ml puromycin (Selleck Chemicals, S7417) or 5 μg/ml blasticidin (Selleck Chemicals, S7419) for one week. Surviving pools were subjected to the indicated experiments.

CRISPR-Cas9 knockout, dox-inducible shRNA, and RNA interference. For CRISPR-Cas9 knockout, sgRNAs targeting Sel1L genes were cloned into the pLenti-spgRNA V2.0-spCas9-Blasticidin plasmid, and then lentiviral vectors were produced as described above. HCT116 and DLD1 cells were infected as described above and treated with 5 μg/ml blasticidin for one week. Surviving cells were plated in 96-well plates at one cell per well for single-colony

selection. The knockout efficiency of Sel1L in cells was assessed by immunoblotting analysis, and disruption of the Sel1L locus was confirmed by Sanger sequencing.

Dox-inducible shVCP cell models were generated according to the protocol described above. In the dox-inducible shVCP experiments, 1 μg/ mL of doxycycline (Selleck Chemicals, S5159) was added and refreshed every three days to induce shRNA expression.

For RNA interference, VCP and HDAC1 siRNAs were purchased from RiboBio (Guangzhou, China) and transfected using Lipofectamine RNAiMAX Transfection (Invitrogen, 13778075) Reagent according to the manufacturer's instructions. The siRNA sequences used are listed in *SI Appendix*, Table S1.

Luciferase reporter assay. Cells expressing VCP or control vector or treated with siVCP were transfected with the luciferase reporter plasmid containing the CPT1A promoter or the control plasmid in the presence of pRLTK (Renilla luciferase control reporter vector). After 48 h of transfection, the cells were lysed and luciferase activity was measured using the Dual-Luciferase Reporter Assay System (Promega, E1910) according to the manufacturer's instructions. Renilla measurements were used to normalize the changes in firefly luciferase activity.

Cell growth, clonogenic assay, and cell proliferation. Cell growth was assessed by serial cell counting using the CellTiter-Glo luminescent assay kit (Promega, G7570) according to the manufacturer's instructions. Luminescence was measured on a Fluostar Omega Reader (BMG Labtech). Cells were seeded in triplicate in 100 μl/well of medium per condition on day 0. The baseline level of luminescence measured on day 0 was subtracted from each corresponding plate at other time points to determine relative cell growth. For clonogenic assays, 1,000 cells per well were seeded in triplicate into 6-well plates and allowed to adhere overnight. Cells were then cultured under different conditions as indicated in the figures. After 10-14 days, the cells were fixed with 4% formaldehyde, stained with Giemsa solution (Keygen, KGA228) according to the manufacturer's instructions, and photographed using a digital scanner (Canon). Colonies were counted using ImageJ software. Cell proliferation was assessed using Click-iT EdU Flow Cytometry Assay kits (Invitrogen, C10425) according to the manufacturer's instructions. Analysis was performed using CytoFLEX (Beckman Coulter) and CytExpert software.

Immunoblotting. Proteins from cells or tumor tissues were extracted using M-PER (Thermo Scientific, 78501) or T-PER (Thermo Scientific, 78510) buffer containing 1 × protease inhibitor cocktail (Topscience, C0004). The BCA Protein Assay Kit (Thermo Scientific, 23225) was used to determine protein concentrations. Protein extracts were separated by sodium dodecyl sulfate-polyacrylamide gel electrophoresis (SDS-PAGE), transferred to polyvinylidene fluoride (PVDF) membranes (Roche, 3010040001), and subjected to immunoblot analysis. The primary antibodies used were: VCP (1:1000, Abcam, ab109240), Sel1L (1 μg/ml, Abcam, ab78298), CPT1A (1:1000, Abcam, ab220789), Histone H3 (1 μg/ml, Abcam, ab176842), Lamin B1 (0.1 μg/ml, Abcam, ab16048), HDAC1 (1:1000, Abcam, ab280198), IRE1 (1:1000, Cell Signaling Technology, 3294), LDHA (1:1000, Cell Signaling Technology, 3582), DYKDDDDK Tag (Flag) (1:1000, Cell Signaling Technology, 14793), alpha-Tubulin (1:10000, Arigo, ARG65693), beta Actin (1:10000, Arigo, ARG65683) and GAPDH (1:10000, Arigo, ARG65680). Goat anti-Rabbit IgG (1:10000, Arigo, ARG65351) or Goat anti-Mouse IgG (1:10000, Arigo, ARG65350) were used for secondary antibodies. Immunoblotting images were captured using a ChemiDoc XRS+ system (Bio-Rad).

Immunoprecipitation. Cells were treated with or without 30 μM MG132 (Selleck Chemicals, S2619) for 6 h prior to harvesting and then lysed in IP lysis buffer (Beyotime, P0013J) containing 1 × protease inhibitor cocktail for 10 min on ice. Soluble lysates were incubated with indicated antibodies at 4°C overnight, and this was followed by incubation with protein A/G magnetic beads (Bimake, B23201) at 4°C overnight. The complexes were boiled in 5 × loading buffer for 10 min and separated from the beads using a magnetic separator. The precipitated proteins were subjected to SDS-PAGE and blotted with specific antibodies to confirm the interaction between VCP and HDAC1. Immunoblotting was performed as previously described.

Ubiquitination assay. For the HDAC1 ubiquitination assay, cells were transfected with plasmids encoding Flag-tagged HDAC1 and HA-tagged ubiquitin using Lipofectamine 3000 Transfection Reagent (Invitrogen, L3000015) according to the manufacturer's instructions. After 24 h, transfected cells were treated with 0.3 μM CB-5083 or siVCP for 24 or 48 h, and the cells were harvested and lysed in 400 μl IP lysis buffer containing 1 × protease inhibitor

cocktail for 10 min on ice. The lysates were incubated with 20 μl of Flag magnetic beads (Bimake, B26101) at 4℃ for 12 h with rotation. After precipitation and elution, the complexes were boiled in 5 × loading buffer for 10 min and separated from the beads using a magnetic separator. Precipitated HDAC1 polyubiquitinated proteins were separated by SDS-PAGE and detected by immunoblotting with an anti-HA antibody. Immunoblotting was performed as previously described.

Immunofluorescence staining. The cells were fixed in 4% paraformaldehyde for 15 min and permeabilized with 0.5% Triton X-100 for 15 min. After, the cells were incubated with primary antibodies overnight at 4°C in a humidifying chamber and then further incubated with the appropriate secondary antibody at room temperature. The primary antibodies used were: VCP (2 μg/ml, Abcam, ab110308), Flag (1:800, Cell Signaling Technology, 14793) and CPT1A (1:100, Abcam, ab220789). The nuclei were counterstained with Hoechst 33342 (Sigma, 14533) prior to mounting. Confocal fluorescence images were captured using Nikon A1 spectral confocal microscope.

Duolink PLA Assay. Duolink PLA assay (Sigma, DUO92101) was performed according to the manufacturer's instructions. Briefly, the cells were fixed with 4% paraformaldehyde for 15 min and permeabilized with 0.1% Triton X-100 diluted in PBS at room temperature. The cells were blocked with 5% BSA, incubated with primary antibodies and PLA probes followed by ligation and amplification using the recommended conditions according to the manual. Antibodies to the following were used: VCP (1:100, Novus, NB120-11433) and HDAC1 (1:2000, Abcam, ab280198). Images were captured as described above.

Subcellular fractionation and salt extractions. Cytosol and nuclear fractions were obtained as described(2). Briefly, cells were lysed in Buffer A (10 mM HEPES, 1 mM KCl, 1.5 mM $MgCl_2$, 0.34 M sucrose, 10% glycerol, 1 mM DTT, 0.25% NP40, and 1 × protease inhibitor cocktail, pH 7.9) for 10 min on ice. After a 10 min centrifugation at 1,300 × g at 4℃, the cytoplasmic fraction (supernatant) was collected. The pellet was then resuspended in Buffer B (3 mM EDTA, 0.2 mM EGTA, 1 mM DTT, and 1 × protease inhibitor cocktail, pH 7.9) and incubated on ice for 10 min with vigorous vortexing three times. The nuclear fraction was collected after a 10 min centrifugation at 1,700 × g at 4℃ to remove the insoluble material and

the processed for immunoblotting (as described above). Salt extraction was performed as previously described(3). Briefly, nuclei from cells that were prepared as described above were suspended in Buffer C (10 mM Tris-HCl, 80M NaCl, 2 mM $MgCl_2$, 2 mM EGTA, 0.1% Triton X-100, and 1 × protease inhibitor cocktail, pH 7.5). They were then sequentially incubated with increasing concentrations of NaCl (80, 200, 400, 600, and 800 mM) and then centrifuged at 400 × g at 4°C for 30 min. Each supernatant (chromatin fraction) was collected and analyzed by immunoblotting (as described above).

Real-Time PCR. Total RNA was extracted using TRIzol according (Invitrogen, 15596026) to the manufacturer's instructions. cDNA was produced from 2 μg of RNA using oligo(dT) (Invitrogen, AM5730G) and RevertAid Reverse Transcriptase (Thermo Scientific, EP0441) according to the manufacturer's instructions. qPCR was performed using an Applied Biosystems 7500 Fast Sequence Detection system with primers and SYBR Green Master Mix. Data were analyzed using the ΔΔCT method with actin as a housekeeping gene. The primer sequences used are listed in *SI Appendix*, Table S1.

Immunohistochemistry. Immunohistochemistry (IHC) was performed as previously described(4). The antibodies used were: Ki67 (1 μg/ml, Abcam, ab15580) and CPT1A (1:100, Abcam, ab220789). Images were captured using an Axio Scan.Z1 microscope (Zeiss). ImageJ software was used for quantification, and the quantitative averages of the three fields were used for statistical analysis.

Lipid droplets staining and quantification. Cells were fixed in 4% paraformaldehyde for 15 min and then stained with 0.5 μg/ml BODIPY 493/503 (Invitrogen, D3922) for 20 min at room temperature while protected from light. The nuclei were counterstained with Hoechst 33342. All images were collected using a confocal microscope (as previously described above). The mean fluorescence intensity (MFI) was determined using ImageJ software.

Measurement of ATP and NADPH/$NADP^+$. Cellular ATP and intracellular NADPH levels were measured using the ATP assay (Beyotime, S0026) and NADPH/$NADP^+$ ratio assay kits (Abcam, ab65349), respectively, according to the manufacturer's instructions.

Metabolism assays. Oxygen consumption rates (OCR) were measured in XF base media under basal conditions and in response to 200 μM etomoxir (Selleck Chemicals, S8244), 1 μM oligomycin (Selleck Chemicals, S1478), 1 μM fluoro-carbonyl cyanide phenylhydrazone (FCCP) (Selleck Chemicals, S8276), and 1 μM rotenone (Sigma, 45656) + 1 μM antimycin A (Sigma, A8674) treatments using a 24-well XFe Extracellular Flux Analyzer (Seahorse Bioscience). Fatty acid oxidation experiments were performed using the XFe Palmitate Oxidation Stress Test Kit (Agilent, 102720-100) according to the manufacturer' instructions. Briefly, the cells were incubated overnight with substrate-limited growth medium (XF DMEM medium with 0.5 mM glucose, 1 mM GlutaMAX, 1% FBS, and 0.5 mM l-carnitine) and then replaced with substrate-limited assay medium (DMEM with 2.0 mM Glucose and 0.5 mM l-carnitine) for analysis. Bovine serum albumin with or without palmitate conjugation (Agilent) was added to the medium for testing of fatty acid oxidation. The data were analyzed using the Seahorse XF Cell Mito Stress Test Report Generator package.

Acylcarnitines analysis. The cells were collected according to a previously published procedure(5). Acylcarnitine analysis was performed at the Technology Center for Protein Sciences at Tsinghua University. A list of the acylcarnitine species is provided in *SI Appendix*, Table S2.

Metabolic tracing analysis of ^{13}C-labeled palmitate. The cells were cultured with 100 μM ^{13}C-labeled palmitic acid (Sigma, 605573) for 24 h. An unlabeled culture was prepared in parallel by adding 100 μM unlabeled palmitic acid (Sigma, P5585) to the media for 24 h to identify unlabeled metabolites. Cells were washed twice with ice-cold PBS and extracted on dry ice with cold 80% methanol in water. The samples were centrifuged at 14,000×g for 20 min at 4 ℃ and supernatants were collected. The extracted metabolites were concentrated completely to dryness using concentrator plus (Eppendorf, Germany). The metabolite residues were re-dissolved in 80% methanol and used for LC-MS/MS analysis. The LC-MS/MS analysis was performed at the Technology Center for Protein Sciences at Tsinghua University. Isotopolog distributions of the metabolites were quantified, normalized to protein and corrected for natural ^{13}C abundance in samples supplemented with ^{12}C-Palmitate. A list of the metabolites is provided in *SI Appendix*, Table S3 and S4.

RNA-sequencing analysis and gene set enrichment analysis (GSEA). To profile the gene expression differences, total RNA was extracted using TRIzol following the manufacturer's instructions and then sent to the Wuhan Genomics Institution (BGI) for RNA-sequencing analysis. The sequencing reads were mapped to the reference genomes (hg38/GRCh38) using HISAT2 software. Fragments per kilobase of transcript per million (FPKM) for each cell line were log2 transformed. DESeq2 was used for differential gene expression analysis. GSEA analysis was implemented using the GSEA software platform with the 'Signal2Noise' metric to generate a ranked list and a 'gene set' permutation type. Gene sets with normal P-values < 0.05 were considered to be statistically significant.

Chromatin immunoprecipitation (ChIP) analysis. ChIP assays were performed using the SimpleChIP Plus Enzymatic Chromatin IP Kit (Cell Signaling Technology, 9005) according to the manufacturer's instructions using antibodies against anti-IgG (1 μg, Abcam, ab172730), anti-Flag (1:50, Cell Signaling Technology, 14793), and anti-VCP (1:100, Abcam, ab109240). Input DNA was used to control for background. The final ChIP DNA sample was used for sequencing analysis and qPCR. For ChIP-sequencing, ChIP DNA was processed for library generation using the QIAseq Ultralow Input Library Kit (QIAGEN, 180492) following the manufacturer's instructions. Libraries were sequenced and analyzed by Epibiotek Co. (Guangzhou, China). Briefly, reads were aligned to the GRCh38/hg38 assembly using Bowtie2. Peak calling was performed using MACS2 to generate the final list of peaks. ChIP was quantified by qPCR using SuperReal PreMix SYBR Green (TIANGEN, FP205) on an Applied Biosystems 7500 Fast Sequence Detection System. Primers used for ChIP-qPCR are listed in *SI Appendix*, Table S1.

Mass spectrometry analysis. VCP and its interacting proteins were immunoprecipitated as described above in the immunoprecipitation assay. The proteins were sent to Applied Protein Technology (Shanghai, China) and subjected to liquid chromatography–tandem mass spectrometry (LC-MS/MS) analysis. The data were analyzed using the Applied Protein Technology.

Quantification and statistical analysis. All data were analyzed using the appropriate statistical methods with GraphPad Prism software. Comparisons between different groups were

evaluated using the Student's t-test (for two groups), one-way ANOVA or two-way ANOVA (for multiple groups) as appropriate. The animal study was randomized by table of random digits. Tumor volume values were analyzed using repeated-measures one-way ANOVA. Data are presented as the mean ± SD or mean ± SEM values of at least three biological replicates unless otherwise stated in the figure legend, and the corresponding P-values for the data are provided in the figure legend. Differences were considered significant if the P value was less than 0.05.

Data analysis on public datasets. Box plot analysis of *VCP* expressions in normal tissues versus tumors was generated from TCGA datasets. Kaplan-Meier survival curves of patients with human tumors generated from GEO datasets via R software. Correlation plots of *VCP* with *CPT1A* expression in human cancer datasets were generated from TCGA datasets via R software.

SI Appendix, Fig. S1.

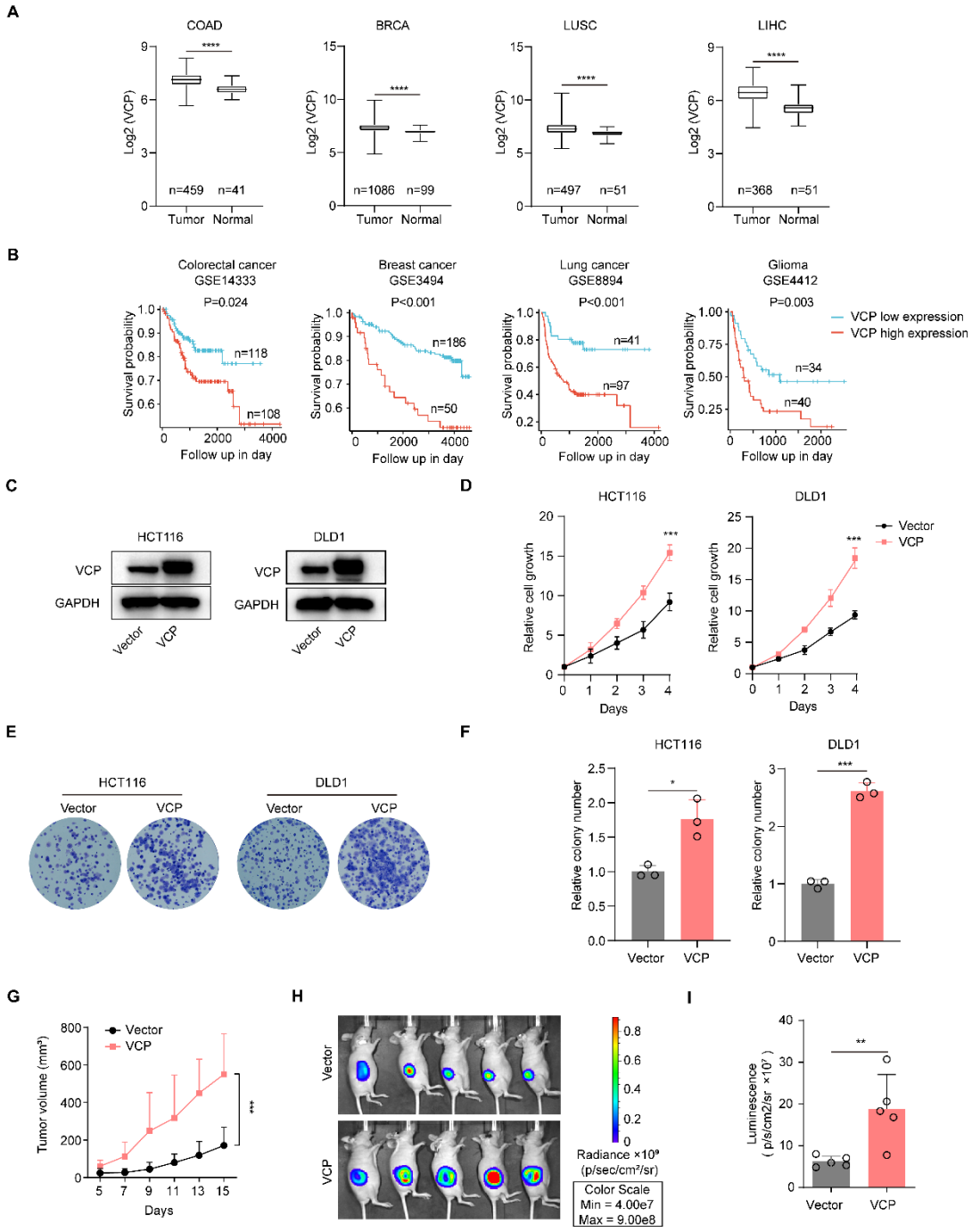

Fig. S1. VCP is overexpressed in human cancers, correlates with poor patient survival, and promotes CRC growth. (A) Box plot comparing transcript levels of *VCP* in tumor and their normal counterparts. Data were generated from TCGA datasets. COAD: Colon adenocarcinoma, BRCA: Breast invasive carcinoma, LUSC: Lung squamous cell carcinoma, LIHC: Liver hepatocellular carcinoma. (B) Kaplan-Meier survival curves of patients with cancer based on *VCP* expression. Data were generated from GEO datasets via 'R2: Genomics Analysis and Visualization Platform'. (C) Western blot checking overexpression of VCP in HCT116 and DLD1 cells. (D) The

relative growth of HCT116 and DLD1 cells stably expressing VCP or control vector. VCP versus Vector at day 4. n=3. (E and F) Colony formation assay of HCT116 and DLD1 cells stably expressing VCP or control vector, and colony number was quantified. n=3. (G) Tumor volume quantification for HCT116-luciferase xenografts stably expressing VCP or control vector in mice. n=5 mice per group. (H and I) Tumor bioluminescence images of mice at the end of the experiment in (G), and luciferase signal intensities were quantified. Data represent mean ± SD. $^{*}P<0.05$, $^{**}P<0.01$, $^{***}P<0.001$, $^{****}P<0.0001$. *P* values were determined by Student's t-test. Tumor volume values were analyzed using repeated-measures one-way ANOVA.

SI Appendix, Fig. S2.

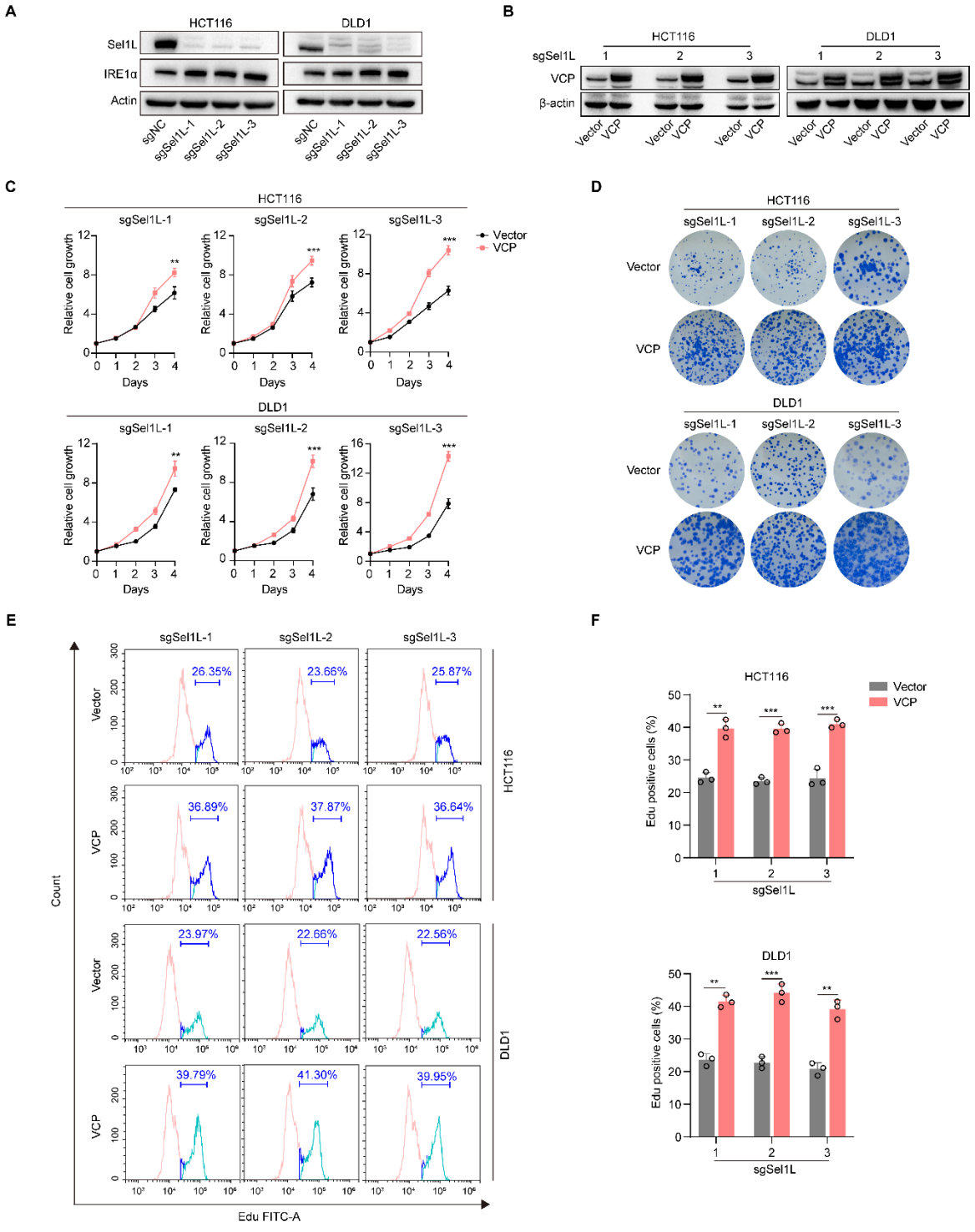

Fig. S2. VCP promotes CRC cell growth in an ERAD-independent manner. (A) Western blot analysis of the indicated proteins in HCT116 and DLD1 cells transfected with sgRNAs targeting Sel1L. (B) Western blot checking the overexpression of VCP in Sel1L-knockout cells. (C) The relative growth of Sel1L-knockout cells stably expressing VCP or control vector. VCP versus Vector at day 4. n=3. (D) Colony formation assay of Sel1L-knockout cells stably expressing VCP or control vector. (E and F) Flow cytometry analysis of EdU incorporation

and PI staining in Sel1L-knockout cells stably expressing VCP or control vector. (F) EdU-positive cells were quantified. n=3. Data represent mean ± SD. $^{**}P<0.01$, $^{***}P<0.001$. *P* values were determined by Student's t-test.

SI Appendix, Fig. S3.

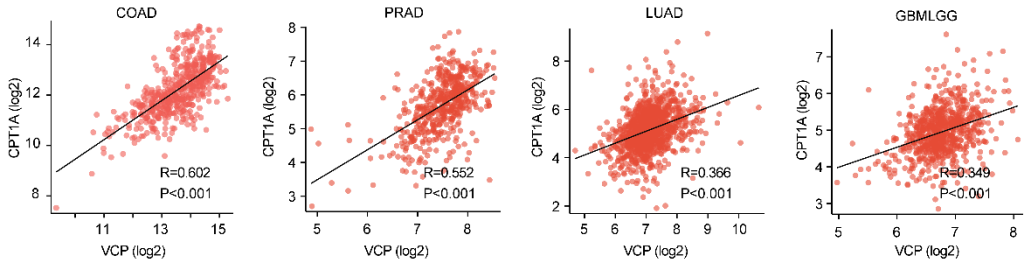

Fig. S3. *VCP* is positively correlated with *CPT1A* expression. Correlation plots of *VCP* expression with *CPT1A* expression with significant Pearson's correlation in tumor datasets are shown. R, Pearson's correlation coefficient; x and y axes denote the respective genes being analyzed. Data were generated from TCGA 'Colon adenocarcinoma' (ID: COAD), 'Prostate adenocarcinoma' (ID: PRAD), 'Lung adenocarcinoma' (ID: LUAD) and 'Glioma' (ID: GBMLGG) datasets via 'R2: Genomics Analysis and Visualization Platform'.

SI Appendix, Fig. S4.

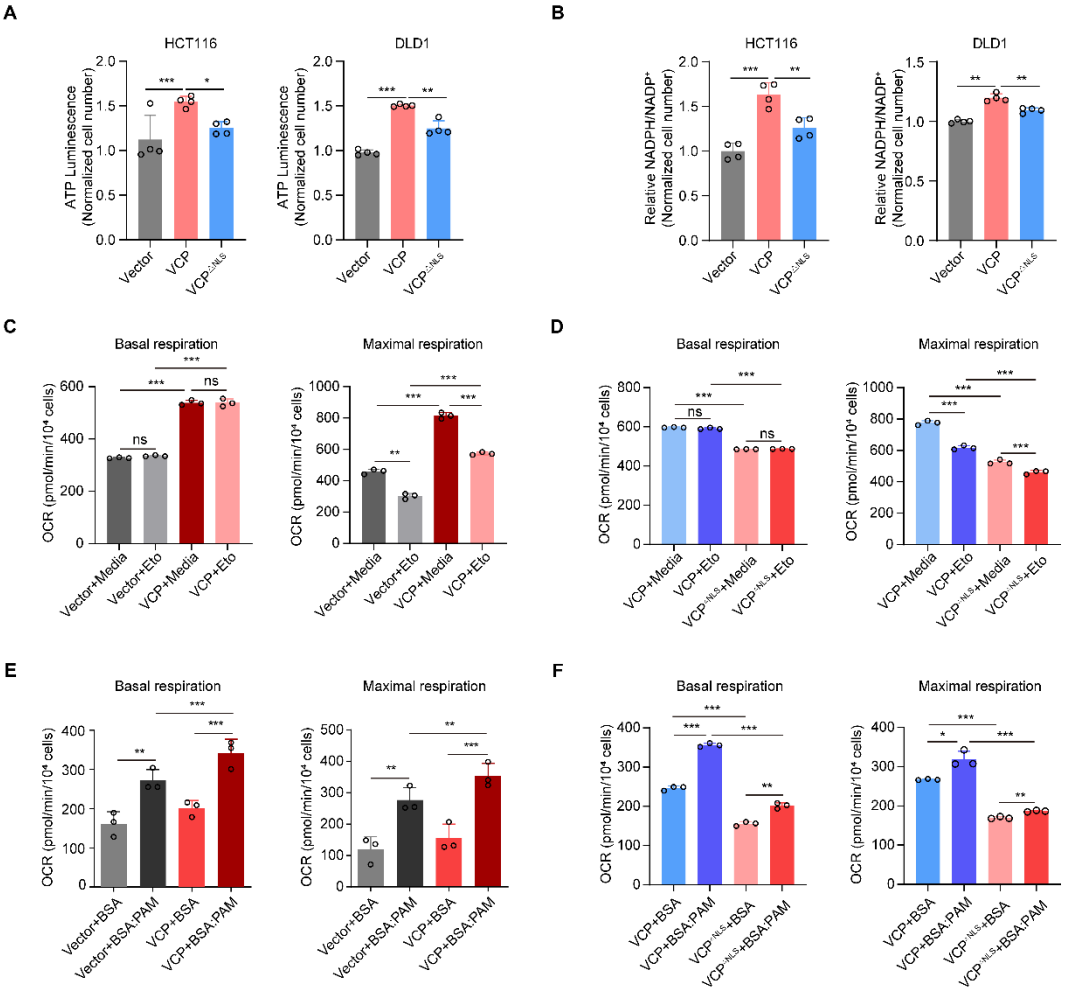

Fig. S4. Nuclear VCP increases FAO capacity in CRC. (A and B) Relative ATP luminescence (A) and NADPH/NADP$^+$ ratios (B) in cells stably expressing VCP, VCP$^{\triangle NLS}$, or control vector. All data were normalized to cell number. n=4. (C-F) Calculation of the basal respiration and maximal respiration in Fig. 3 (F, H, J, and L). n=3. Data represent mean ± SD. ns: not significant, $^{*}P<0.05$, $^{**}P<0.01$, $^{***}P<0.001$. *P* values were determined by one-way ANOVA.

SI Appendix, Fig. S5.

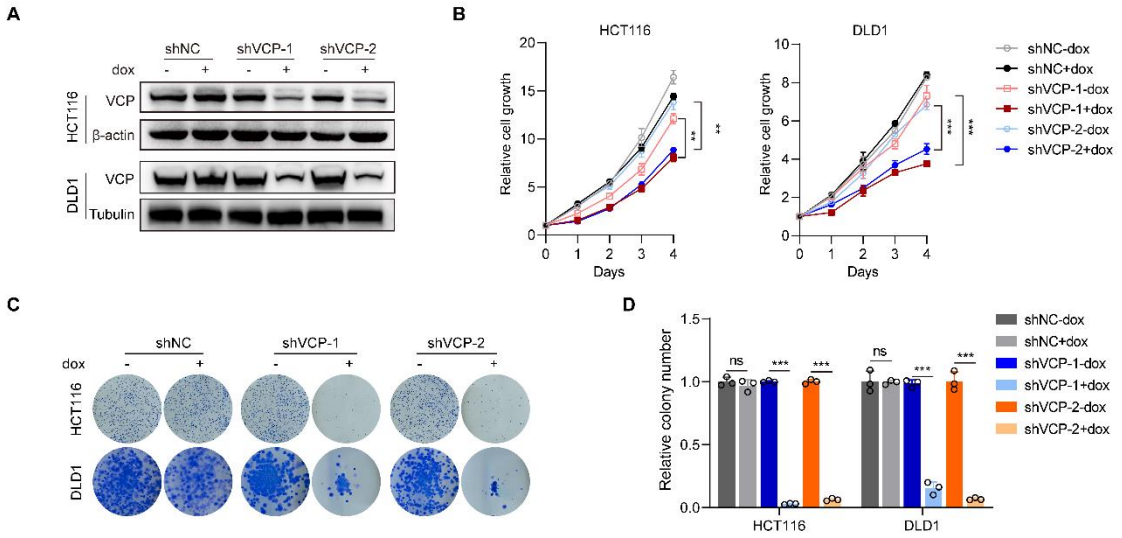

Fig. S5. Knockdown of VCP inhibits CRC cell growth. (A) Western blot analysis of cells transfected with dox-inducible shRNA in the absence or presence of dox. (B) The relative growth of cells transfected with dox-inducible shVCP or shNC in the absence or presence of dox. shVCP-dox versus shVCP+dox at day 4. n=3. (C and D) Colony formation assay of cells transfected with dox-inducible shVCP or shNC in the absence or presence of dox. (D) Colony number was quantified. n=3. Data represent mean ± SD. ns: not significant, $^{**}P<0.01$, $^{***}P<0.001$. *P* values were determined by one-way ANOVA.

***SI Appendix*, Fig. S6.**

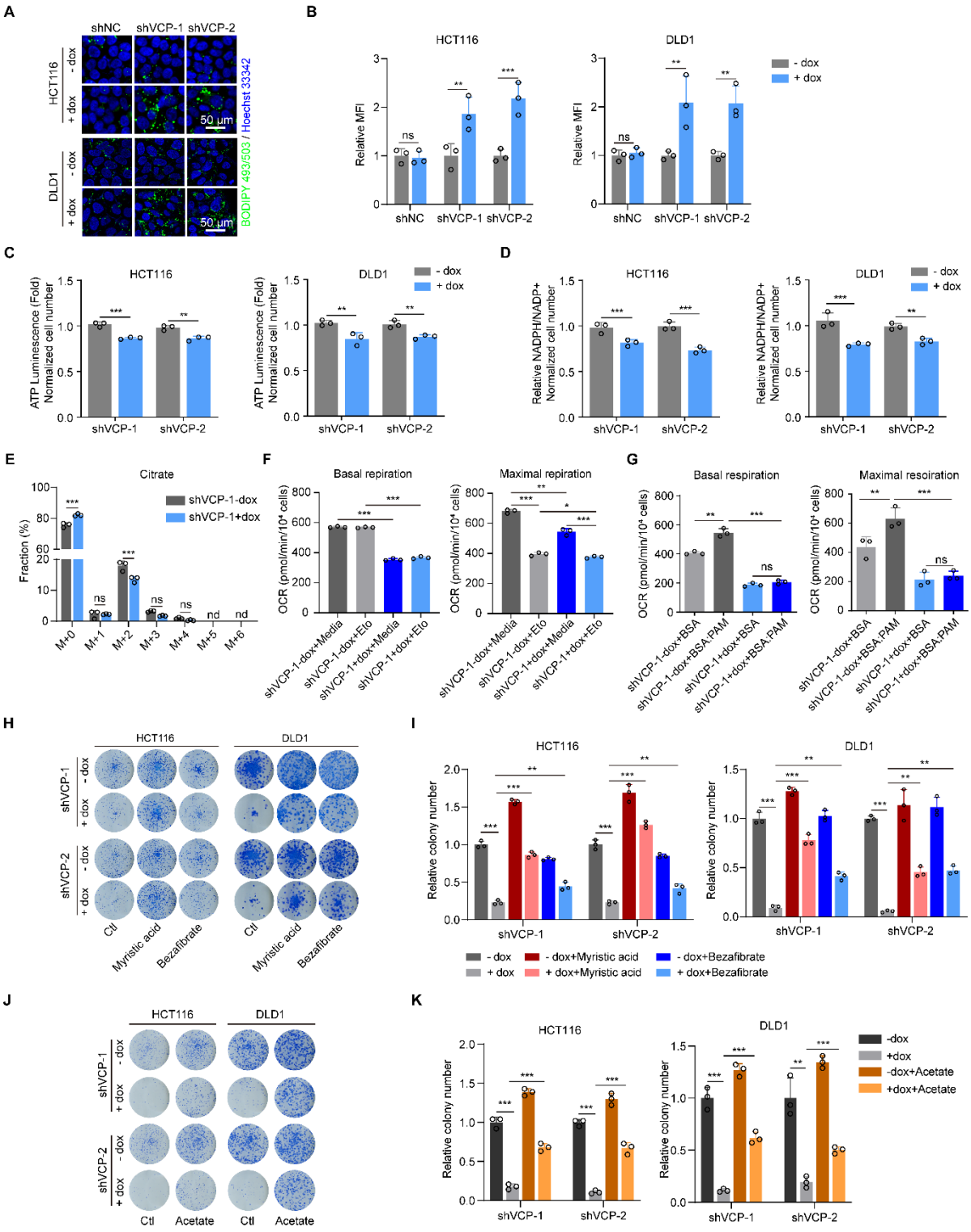

Fig. S6. Knockdown of VCP inhibits FAO, which impaired CRC cell growth. (A and B) BIODIPY 493/503 staining was used to determine the content of lipid droplets in cells transfected with dox-inducible shVCP in the presence or absence of dox. Scale bar, 50 μm. (B) The mean fluorescence intensity (MFI) was quantified. n=3. (C

and D) Relative ATP luminescence (C) and NADPH/NADP+ ratios (D) in HCT116 and DLD1 cells transfected with dox-inducible shVCP in the presence or absence of dox. All data were normalized to cell number. n=3. (E) Metabolic tracing analysis of ^{13}C-labeled palmitate in HCT116 cells transfected with dox-inducible shVCP in the absence or presence of dox. The fraction of each isotopomer for the citrate pool is shown. (F and G) Calculation of the basal respiration and maximal respiration in Fig. 4 (C and E). n=3. (H and I) Colony formation assay of cells transfected with shVCP in the presence or absence of dox after the indicated treatments with myristic acid (10 μM) or bezafibrate (5 μM). (I) Colony number was quantified. n=3. (J and K) Colony formation assay of cells transfected with dox-inducible shVCP in the presence or absence of dox after the indicated treatments with acetate (10 μM). (K) Colony number was quantified. n=3. Data represent mean ± SD. ns: not significant, nd: not detected, $^{*}P<0.05$, $^{**}P<0.01$, $^{***}P<0.001$. *P* values were determined by Student's t-test for (B, C, D and E) or one-way ANOVA for (F,G, I and K).

SI Appendix, Fig. S7.

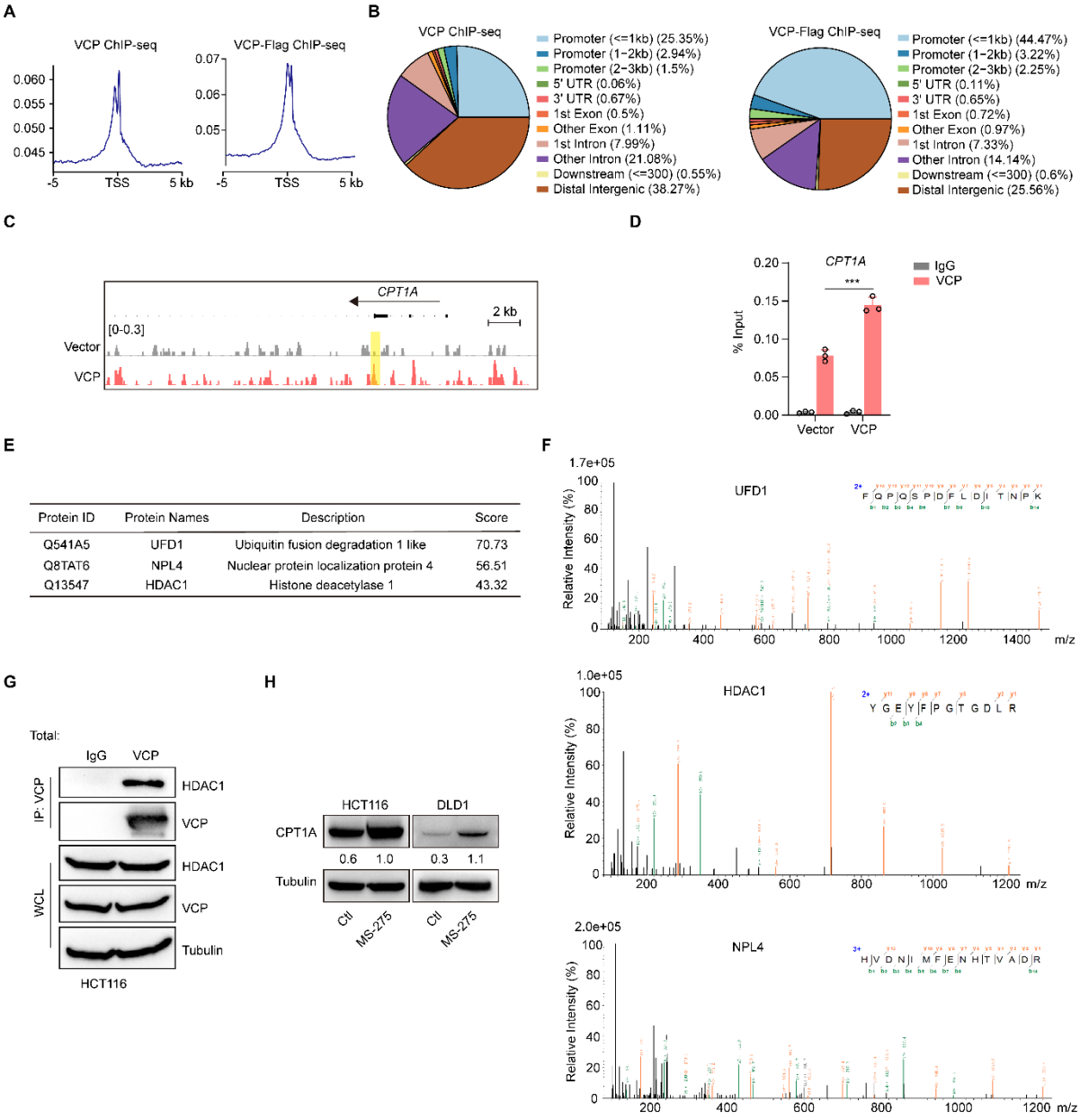

Fig. S7. VCP binds to the promoter of *CPT1A* and regulates its transcription via HDAC1. (A) Average position of VCP and Flag-VCP binding peaks within 5 kb of the gene transcription start sites (TSS) determined by ChIP-seq analysis of HCT116 cells stably expressing VCP or Flag-tagged VCP. (B) Composition of VCP and Flag-VCP binding peaks. UTR, untranslated region. <=1 kb and -1 kb to +1 kb from TSS; 1–2 kb, 2 to 1 kb, and +1 to +2 kb from TSS; and 2–3 kb, 3 to 2 kb, and +2 to +3 kb from TSS are shown. (C) Representative ChIP-seq signal (*CPT1A* locus) for VCP in HCT116 cells stably expressing VCP or vector control. The yellow aera represent the binding site of VCP in the promoter of *CPT1A*. (D) ChIP-qPCR analysis of VCP binding to the *CPT1A* promoter in HCT116 cells stably expressing VCP or vector control. DNA enrichment was calculated as

percentage of input, with normal IgG as control. n=3. (E and F) Flag-tagged VCP was immunoprecipitated from HCT116 cells stably expressing Flag-tagged VCP and subjected to mass spectrometry analysis. (F) The product ion (MS/MS) spectra obtained for cross-linked peptides of UFD1, NPL4 and HDAC1. (G) Total cell lysates from HCT116 cells treated with MG-132 were collected for IP with either nonspecific IgG or with an antibody against VCP, and immunoblotted as indicated. WCL, whole cell lysates. (H) Western blot analysis of CPT1A in cells treated with MS-275 (HCT116, DLD1: 2 μM) for 24 h. Data represent mean ± SD. $^{***}P<0.001$. *P* values were determined by two-way ANOVA.

SI Appendix, Fig. S8.

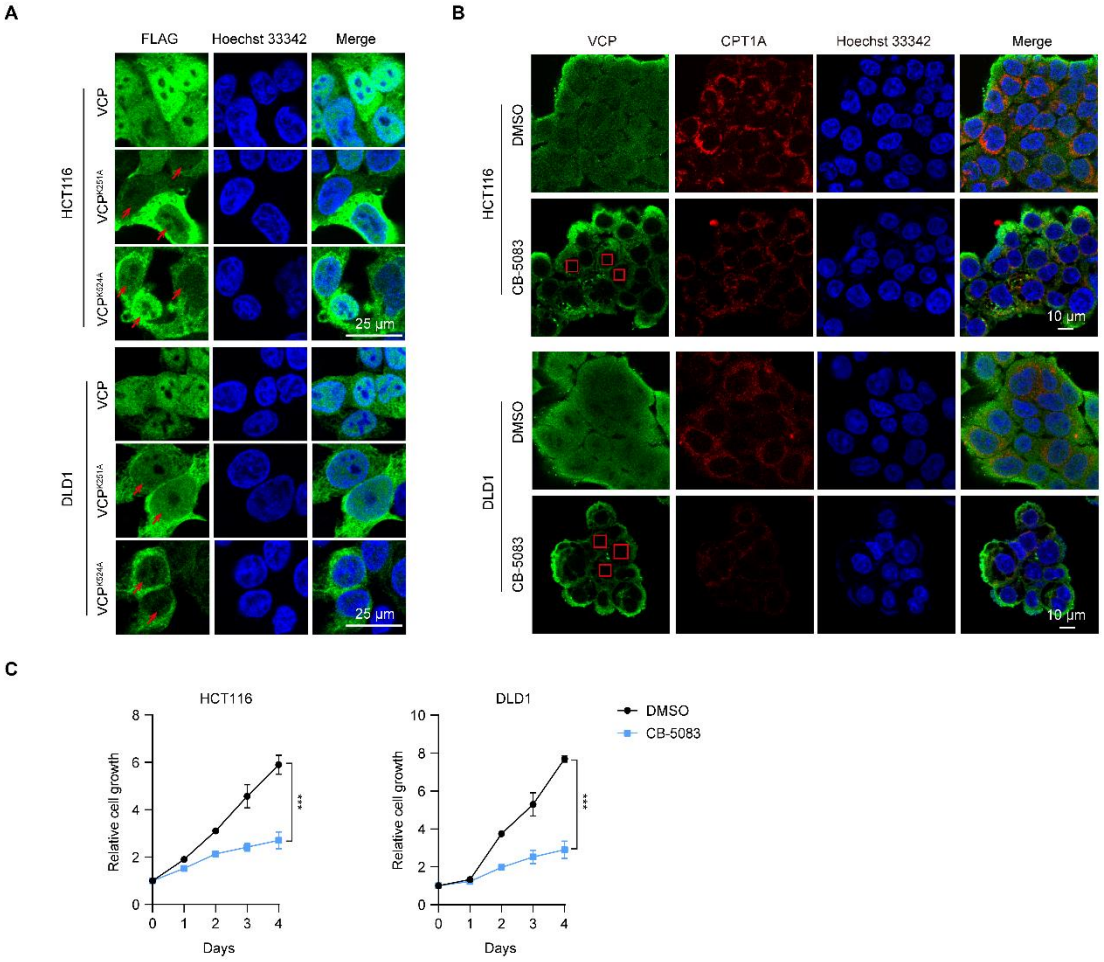

Fig. S8. CB-5083 decreases nuclear VCP levels and inhibits CRC cell growth. (A) HCT116 and DLD1 cells were transfected with Flag-tagged VCP, VCP^{K251A} or VCP^{K524A}, followed by immunofluorescent staining for Flag (green) and Hoechst 33342 (blue). Red arrows depict the nuclear VCP localization. Scale bar, 25 μm. (B) Immunofluorescent staining of VCP (green) and CPT1A (red) in HCT116 and DLD1 cells treated with or without CB-0583 (HCT116, 0.3μM; DLD1, 1μM) for 24 h. Red boxes depict the nuclear VCP localization. Scale bar, 10 μm. (C) The relative growth of cells treated with CB-5083 (HCT116, 0.1 μM; DLD1, 0.2 μM) for the indicated time. n=3. Data represent mean ± SD. $^{***}P<0.001$. Cell growth values were analyzed using repeated-measures one-way ANOVA.

SI Appendix, Fig. S9.

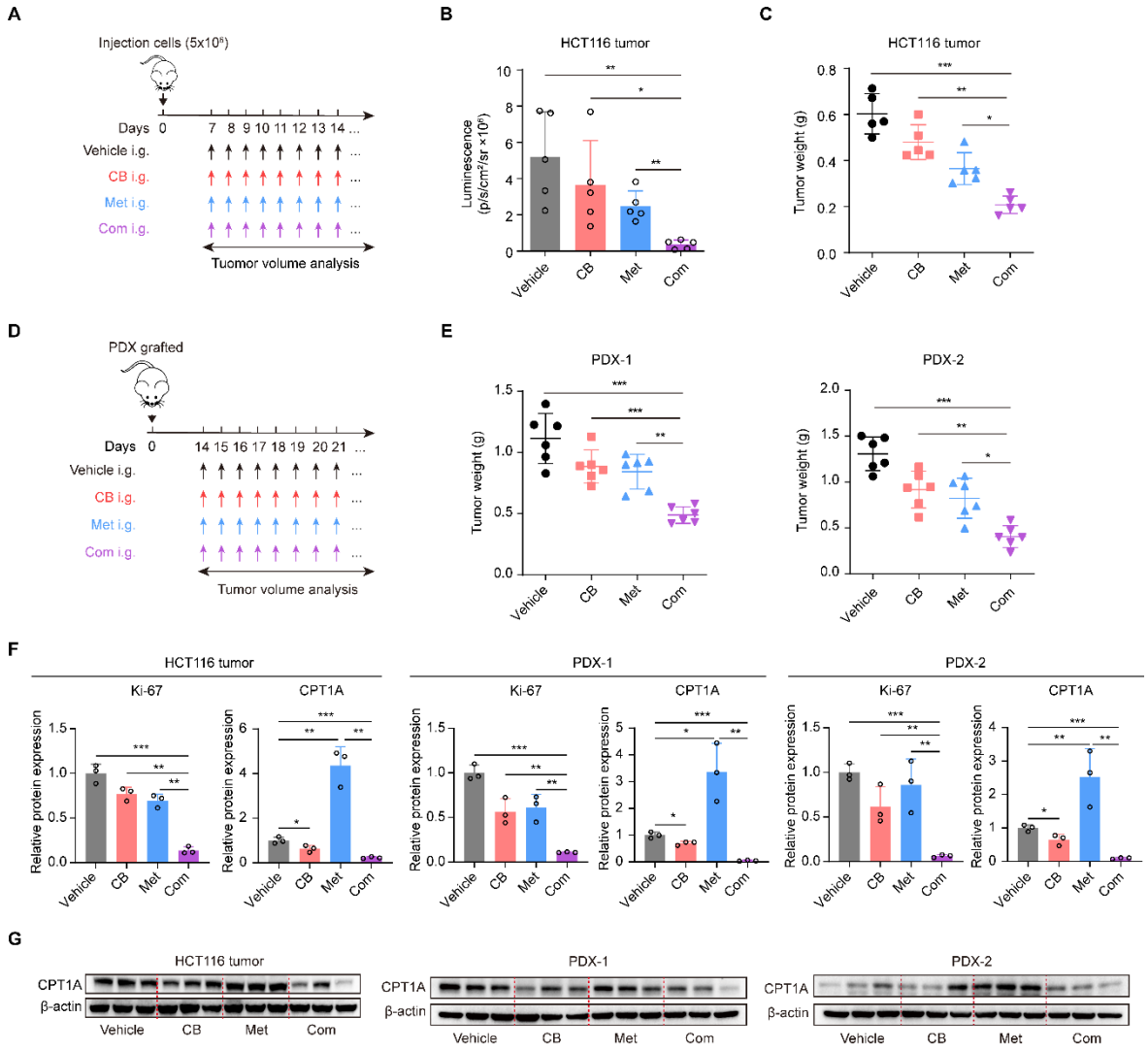

Fig. S9. CB-5083 treatment potentiates the anti-tumor activity of metformin in vivo. (A) Timeline of the experimental setup for Fig. 7A. (B) Quantification of luciferase signal intensities in Fig. 7B. n=5 mice per group. (C) Tumor tissues from Fig. 7A were weighed at the end of experiments. n=5 mice per group. (D) Timeline of the experimental setup for Fig. 7C. (E) Tumor tissues from Fig. 7C were weighed at the end of experiments. n=5 mice per group. (F) Percentage of positively stained cells in Fig.7D was quantified. n=3 mice per group. (G) Western blot analysis of CPT1A in tumor tissues from Fig.7 (A and C). n=3 mice per group. CB: CB-5083, Met: metformin, Com: Combination. Data represent mean ± SD. $^{*}P<0.05$, $^{**}P<0.01$, $^{***}P<0.001$. *P* values were determined by one-way ANOVA.

***SI Appendix*, Table S1. The sequence of oligonucleotides used in this paper**

shRNA and siRNA sequences	**Sequence (5'-3')**	
VCP shRNA1	GGAAGCAGCTAGCTCAGAT	
VCP shRNA2	GCAACCTTCGTAAAGCCTT	
VCP siRNA1	GGAGGTAGATATTGGAATT	
VCP siRNA2	GGCCAAAGCCATTGCTAAT	
HDAC1 siRNA1	GCGACTGTTTGAGAACCTT	
HDAC1 siRNA2	GGGATCGGTTAGGTTGCTT	
HDAC1 siRNA3	AGGCGGTGGTTACACCATT	
qPCR primers	**F- Forward primer sequences (5'-3')**	**R- Reverse primer sequence (5'-3')**
h. *VCP*	CAAACAGAAGAACCGTCCCAA	TCACCTCGGAACAACTGCAAT
h. *PPARG*	AGAAGCCTGCATTTCTGCAT	TCAAAGGAGTGGGAGTGGTC
h. *CPT1A*	GATCCTGGACAATACCTCGGAG	CTCCACAGCATCAAGAGACTGC
h. *CPT2*	GCAGATGATGGTTGAGTGCTCC	AGATGCCGCAGAGCAAACAAGTG
h. *ACADSB*	GCCACCTATTTGCCTCAGCTCA	GCTCAGCACTGCTGATCCACAT
h. *ACADVL*	TAGGAGAGGCAGGCAAACAGCT	CACAGTGGCAAACTGCTCCAGA
h. *ACADM*	ACAGGGGTTCAGACTGCTATT	TCCTCCGTTGGTTATCCACAT
h. *ETFDH*	GGAAACACCATCCTAGCATTCGG	CCACCAGGAAAGGTGAGTTTTGG
h. *ACTB*	GATCATTGCTCCTCCTGAGC	ACTCCTGCTTGCTGATCCAC
gRNA sequences	**Sequence (5'-3')**	
Sel1L gRNA no.1	ACTGCAGGCAGAGTAGTTGC	
Sel1L gRNA no.2	GACATCAGATGAGTCAGTAA	
Chip-qPCR primers	**F- Forward primer sequences (5'-3')**	**R- Reverse primer sequence (5'-3')**
h. *CPT1A*	TAGCTTTCAGCTTAATCCTTTCCT TTTGGCAGAGTA	ATGGCCAGTGCTCAGAAAAGGGA GATG

SI Appendix, Table S2. List of acylcarnitine species

VCP-overexpression			
Compound name	**Acylcarnitines**	**Empirical Formula**	**m/z (Expected)**
L-Carnitine	C7:1	C7H15NO3	162.11247
L-Acetylcarnitine	C9:2	C9H17NO4	204.1230
Propionylcarnitine	C10:2	C10H19NO4	218.13868
Butyrylcarnitine	C11:2	C11H21NO4	232.15433
Isobutyryl carnitine	C11:2	C11H21NO4	232.1544
Hydroxybutyrylcarnitine	C11:2	C11H11NO5	248.1498
Succinylcarnitine	C11:3	C11H19NO6	262.12906
2-Ethylacrylylcarnitine, Tiglylcarnitine	C12:3	C12H21NO4	244.15436
2-Methylbutyroylcarnitine	C12:2	C12H23NO4	246.17053
2-Methylbutyroylcarnitine; 3-Methylbutyrylcarnitine	C12:2	C12H23NO4	246.17053
Pivaloylcarnitine	C12:2	C12H23NO4	246.17053
3-Hydroxyisovalerylcarnitine	C12:2	C12H24NO5+	262.16492
Hydroxyhexanoycarnitine	C13:2	C13H25NO5	276.1811
L-Octanoylcarnitine	C15:2	C15H29NO4	288.21696
3-hydroxyoctanoyl carnitine	C15:2	C15H29NO5	304.2124
Elaidic carnitine,Vaccenyl carnitine	C25:2	C25H47NO5	426.35781
DL-Stearoylcarnitine	C25:2	C25H49NO4	428.37346
Dox-inducible shVCP			
Compound name	**Acylcarnitines**	**Empirical Formula**	**m/z (Expected)**
L-Acetylcarnitine	C9:2	C9H17NO4	204.12303
Hydroxybutyrylcarnitine	C11:2	C11H21NO5	248.1498
Decanoylcarnitine	C17:2	C17H33NO4	316.24824
3-hydroxydecanoyl carnitine	C17:2	C17H33NO5	332.2437
Dodecanoylcarnitine	C19:2	C19H37NO4	344.27954
lauroylcarnitine	C19:2	C19H37NO4	344.27954
cis-5-Tetradecenoylcarnitine	C21:3	C21H39NO4	370.29521
Myristoylcarnitine	C21:2	C21H41NO4	372.31084
Tetradecanoylcarnitine	C21:2	C21H41NO4	372.31086
trans-Hexadec-2-enoyl carnitine	C23:3	C23H43NO4	398.32651
L-Palmitoylcarnitine	C23:2	C23H45NO4	400.34214
3-Hydroxy-9-hexadecenoylcarnitine	C23:3	C23H43NO5	414.32195
3-Hydroxyhexadecanoylcarnitine	C23:2	C23H45NO5	416.3376
Heptadecanoyl carnitine	C24:2	C24H47NO4	414.35781
DL-Stearoylcarnitine	C25:2	C25H50NO4	428.37346
3-Hydroxy-11Z-octadecenoylcarnitine	C25:3	C25H47NO5	442.35325

***SI Appendix*, Table S3. Intensity of TCA metabolites in ^{13}C-labeled palmitate isotope tracing**

VCP-overexpression							
Metabolites	**Isotope**	**Vector**			**VCP**		
Citrate	M+2	259450.4	217570.7	124593.9	404743.4	465411.4	501446.6
Aconitate	M+2	47199.5	30191.8	26034.4	61005.8	83156.9	65953.6
α-KG	M+2	35481.6	26484.2	10266.8	49531.7	57338.9	62842.1
Succinate	M+2	6727.2	8049.9	8469.3	17014.7	17791.7	17138.7
Malate	M+2	47682.8	54361.4	39769.2	82667.4	102614.0	121810.7
Dox-inducible shVCP							
Metabolites	**Isotope**	**shVCP-dox**			**shVCP+dox**		
Citrate	M+2	867821.3	689017.0	782208.1	466331.7	388123.2	285525.5
Aconitate	M+2	152067.1	96511.3	122531.6	67401.4	62135.5	72549.9
α-KG	M+2	114350.1	87370.1	82322.4	55348.4	60175.4	37623.9
Succinate	M+2	36610.8	27424.7	27518.0	20191.5	23081.7	26180.6
Malate	M+2	251916.5	187316.8	188850.6	148907.4	114803.1	143617.8

***SI Appendix*, Table S4. Fraction of each isotopomer for the citrate pool in ^{13}C-labeled palmitate isotope tracing**

VCP-overexpression							
Metabolites	**Isotope**	**Vector (%)**			**VCP (%)**		
Citrate	M+0	90.97	90.21	90.95	87.86	88.01	87.48
	M+1	0.57	1.30	0.83	3.21	1.40	1.44
	M+2	7.81	7.69	7.27	8.40	9.74	10.17
	M+3	0.65	0.80	0.95	0.53	0.85	0.91
	M+4	0	0	0	0	0	0
	M+5	0	0	0	0	0	0
	M+6	0	0	0	0	0	0
Dox-inducible shVCP							
Metabolites	**Isotope**	**shVCP-dox (%)**			**shVCP+dox (%)**		
Citrate	M+0	74.07	76.13	76.85	83.05	81.61	81.87
	M+1	2.97	0.75	2.94	2.38	2.23	2.12
	M+2	18.7	18.98	16.14	12.49	14.07	14.14
	M+3	2.94	3.38	3.28	1.61	1.88	1.67
	M+4	1.32	0.76	0.79	0.47	0.21	0.20
	M+5	0	0	0	0	0	0
	M+6	0	0	0	0	0	0

SI References

1. K. Li *et al.*, ILF3 is a substrate of SPOP for regulating serine biosynthesis in colorectal cancer. *Cell Res* **30**, 163-178 (2020).
2. J. Mendez, B. Stillman, Chromatin association of human origin recognition complex, cdc6, and minichromosome maintenance proteins during the cell cycle: assembly of prereplication complexes in late mitosis. *Mol Cell Biol* **20**, 8602-8612 (2000).
3. E. Meshorer *et al.*, Hyperdynamic plasticity in pluripotent embryonic of chromatin proteins stem cells. *Developmental Cell* **10**, 105-116 (2006).
4. X. Xiao *et al.*, DNA-PK inhibition synergizes with oncolytic virus M1 by inhibiting antiviral response and potentiating DNA damage. *Nat Commun* **9**, 4342 (2018).
5. L. Liu *et al.*, Triose Kinase Controls the Lipogenic Potential of Fructose and Dietary Tolerance. *Cell Metabolism* **32**, 605-+ (2020).